PNAS

Supporting Information for

Hfq-licensed RNA-RNA interactome in *Pseudomonas aeruginosa* reveals a keystone sRNA

Michael J. Gebhardt, Elizabeth A. Farland, Pallabi Basu, Keven Macareno, Sahar Melamed, Simon L. Dove

Corresponding authors:

Michael J. Gebhardt
Email: michael-gebhardt@uiowa.edu

Simon L. Dove
Email: Simon.Dove@childrens.harvard.edu

This PDF file includes:

Supplemental Materials & Methods
Figures S1 to S9
Tables S1 to S5
Legends for Datasets S1 to S2
SI References

Other supporting materials for this manuscript include the following:

Datasets S1 to S2

Supplemental Materials & Methods

Plasmid Construction. Plasmids were constructed using isothermal assembly (ITA) (1). Briefly, plasmids were digested with the appropriate restriction enzymes (New England Biolabs, Ipswitch, MA) and purified. PCR products were amplified using the primers indicated in Supplemental Table S3 using KODX polymerase (Millipore Sigma), resolved via agarose electrophoresis and extracted using Qiagen Gel Extraction columns according to the manufacturer's recommendations. The purified PCR products and linearized vectors were combined in an isothermal assembly reaction on ice, incubated at 50˚C for 15-30 minutes, and transformed by heat-shock into chemically competent DH5α F′IQ cells. The resulting plasmids were confirmed by sequencing (Genewiz/Azenta) prior to use in *P. aeruginosa*.

Plasmid pKH6 (2) was a gift from Steven Lory and allows for arabinose-inducible expression of sRNAs. Plasmid pKH6-PhrS (pPhrS herein) has been described previously (3). For the derivatives described here, the pKH6 backbone was linearized by digestion with XbaI and HindIII. Plasmid pRyhB was created by amplifying a fragment containing *ryhB* from *E. coli* MG1655 using primers RyhB_fwd and RyhB_rev and cloning into pKH6 by ITA. The panel of pPhrS-SM-mutant plasmids were created by combining linearized pKH6, a PCR product created with primers P1_PhrS_alleles and P2_PhrS_SM171-172 or P2_PhrS_SM173-182, and a PCR product created with P4_PhrS_alleles and each individual P3_PhrS-SM alleles by ITA. Plasmid pPhrS-Δseed was created by combining linearized pKH6, a PCR product generated with primers P1_PhrS alleles and P2_PhrSΔseed, and a PCR product created with P3_PhrSΔseed and P4_PhrS_alleles by ITA. Plasmid pPhrSΔ1/2seed was created by combining 10 ng of the pKH6.PhrS-Δ1/2seed gBlock with linearized pKH6 backbone via ITA. Plasmid pKH6-PhrS-mini was created by amplifying a fragment containing only nucleotides 161-213 of *phrS* using primers PhrS-mini_fwd and P4_PhrS_alleles and cloning via ITA into pKH6.

Plasmids pME6014 and pME6016 (4) were a kind gift from Christoph Keel. These plasmids encode a multiple cloning site upstream of a *lacZ* fragment starting at the 8th codon (plasmid pME6014) or upstream of *lacZ* and its ribosome binding site (pME6016), allowing for the creation of translational and transcriptional *lacZ* fusions, respectively. All derivatives of pME6014 and pME6016 described herein were created by ITA with pME6014 or pME6016 plasmids that had been linearized by digestion with EcoRI and PstI. Plasmid pME6014-*hmgA* contains an in-frame translational fusion and was created by amplifying a 699-bp region including the 5' UTR and up to the 61st nt of *hmgA* with primers *hmgA*_reporters_fwd and *hmgA*_translational_rev. Plasmid pME6014-*hmgA-SMC175* contains the same translational fusion as pME6014-*hmgA* with a dinucleotide mutation (GC changed to GC) at positions -58/-57 relative to the *hmgA* start codon that is predicted to restore base-pairing with the PhrS-SM175 allele. PCR fragments were generated from PAO1 genomic DNA with primers *hmgA*_reporters_fwd & *hmgA-SM175C*_rev and *hmgA-SM175C*_fwd & *hmgA*_translational_rev and introduced into linearized pME6014 via ITA. Plasmid pME6014-*PA3340* contains an in-frame translational fusion and was created by amplifying a 466-bp region including the 5' UTR and up to the 46th nt of *PA3340* with primers *PA3340*_reporters_fwd and *PA3340*_translational_rev. Plasmid pME6014-*antR* contains an in-frame translational fusion and was created by amplifying a 441-bp region including the 5' UTR and up to the 46th nt of *antR* with primers *antR*_reporters_fwd and *antR*_translational_rev. Plasmid pME6014-*antR-M2C* contains the same in-frame translational fusion as pME6014-*antR* with a dinucleotide mutation (CC changed to GG) at positions -23/-24 relative to the *antR* start codon that is predicted to restore base-paring with the PhrS-SM179 allele. PCR fragments were generated from PAO1 genomic DNA with primers *antR*_reporters_fwd & P2_*antR*_M2C and P3_*antR*_M2C & *antR*_reporters_rev and introduced into linearized pME6014 via ITA. Plasmid pME6016-*hmgA* was created using the same forward primer as used for pME6014-*hmgA* and a reverse primer, *hmgA*_transcriptional_rev, ending at -89 bp relative to the *hmgA* start codon. Plasmid pME6016-*PA3340* was created using the same forward primer as used for pME6014-*PA3340* and a reverse primer, *PA3340*_transcriptional_rev, ending at -69 bp relative to the *PA3340* start codon. Plasmid pME6016-*antR* was created using the same forward primer as used for pME6014-*antR* and a reverse primer, *antR*_transcriptional_rev, ending at -91 bp relative to the *antR* start codon.

Plasmid pEXG2 is an allele exchange vector used to create chromosomal mutations (5). All pEXG2 derivatives created herein were constructed using ITA with plasmid pEXG2 that had been linearized with HindIII and KpnI. Plasmid pEXG2.*antR*-V was used to create a chromosomally encoded *antR* allele specifying the Vesicular Stomatitis Virus-G protein epitope (VSV-G) and was created by combining linearized pEXG2 plasmid with PCR products created by amplification of PAO1 genomic DNA with primers P1_*antR*-VSVG & P2_*antR*-VSVG and primers P3_*antR*-VSVG & P4_*antR*-VSVG. Plasmid pEXG2.*phrS*-SM179 was used to introduce the PhrS-SM179 allele at the chromosomal locus and was created by combining linearized pEXG2 plasmid with PCR products created by amplification of PAO1 genomic DNA with primers P1_*phrS*-SM179_chrom & P2_*phrS*-SM179_chrom

and P3_*phrS*-SM179_chrom & P4_*phrS*-SM179_chrom. Plasmid pEXG.*antR*-M2C was used to introduce the M2C compensatory mutations to restore interaction with the PhrS-SM179 allele and was created by combining linearized pEXG2 plasmid with PCR products created by amplification of PAO1 genomic DNA with primers P1_*antR*_M2C & P2_*antR*_M2C and P3_*antR*_M2C & P4_*antR*_M2C.

Introduction of Plasmids to *P. aeruginosa.* Replicating plasmids were routinely introduced to *P. aeruginosa* PAO1 and its derivatives by electroporation (pKH6, pME6014, pME6016, and derivatives thereof) using electrocompetent *P. aeruginosa* cells. Electrocompetent *P. aeruginosa* cells were created by pelleting overnight cultures (1.5 mL) at full speed in a tabletop microcentrifuge. The supernatant was removed, the cell pellet was washed thrice with 1 mL of 0.3 M sucrose. The final cell pellet was suspended in approximately 400 µL 0.3 M sucrose. Aliquots (≈70 µL) of electrocompetent cells were mixed with plasmid DNA (routinely 50-100 ng), and electroporated at 1.8 kV in a 2-mm gap electroporation cuvette (VWR). Cells were recovered in LB for 1 hour with shaking at 37˚C prior to plating on the appropriate selective media.

Strain Construction. *E. coli* SM10 (λpir) cells carrying the appropriate pEXG2 derivative plasmid were mated with recipient *P. aeruginosa* cells for 4 hours at 37˚C. Primary integrants were isolated on *Pseudomonas* Isolation Agar (PIA, Difco) containing 60 µg/ml gentamicin. The resulting merodiploid cells were plated on low salt LB plates containing 5% (w/v) sucrose for *sacB* counterselection to select for clones that had resolved the pEXG2 plasmid. Cells were then patched to confirm antibiotic sensitivity and screened by colony PCR and/or sequencing to identify clones containing the desired mutation.

RIL-seq Experiment.

RIL-seq Experimental Procedure.

RIL-seq was performed as described previously (6). Triplicate overnight cultures of PAO1 and PAO1 Hfq-V were back-diluted to an OD_{600} of 0.01 and cultures were grown until exponential phase (OD_{600} ≈ 0.5) and early stationary phase (OD_{600} ≈ 2). At each time point, the equivalent of 40 OD units were removed from the culture flasks and processed for RIL-seq. Cells were pelleted, washed twice with ice-cold PBS, and treated with 80,000 µJ/cm^2 of 254 nm UV irradiation. Cells were disrupted via bead beating and a portion of the cell lysate was retained for the total RNA RNA-seq samples. Hfq-RNA complexes were immune precipitated with a monoclonal anti-VSVG antibody (Sigma Aldrich part number SAB4200695) from the remaining cell lysate. Following immunoprecipitation, RNA ends were trimmed with RNAse A/T1 (Thermo Fisher Scientific, cat. no. EN0551), phosphorylated with T4 Polynucleotide Kinase (NEB, cat. no. M0201), subjected to ligation using T4 RNA Ligase 1 (NEB, cat. no. M0437M) and treated with proteinase K. RNAs were then extracted with TriReagent LS (Sigma-Aldrich) according to the manufacturer's recommendations. Subsequently, the RIL-seq and corresponding total RNA samples were prepared for Illumina sequencing using the RNAtag-seq protocol (7) with adaptations to capture bacterial sRNAs (6). Ribosomal RNAs were depleted using the Ribo-Zero Plus rRNA depletion kit (Illumina cat. no. 20040526). The final libraries were sequenced by paired-end sequencing at the Harvard Medical School Biopolymers facility on a NextSeq500 sequencer (Illumina). RNA/cDNA quality was assessed at various stages of library construction by the Molecular Genetics Core facility at Boston Children's Hospital.

Computational Analysis of RIL-seq.

The RIL-seq analysis was carried out as described (6) with modifications to the pipeline for the *P. aeruginosa* genome. The RIL-seq software package (version 0.78) was downloaded from github at: https://github.com/asafpr/RILseq. Raw sequencing reads were processed to remove adaptor sequences, low complexity reads, and low-quality ends using cutadapt version 2.10 (8). The first 25 nucleotides of each read were then mapped to the *P. aeruginosa* PAO1 genome (GenBank: NC_002516.2) using the 'map_single_fragments.py' program included in the RIL-seq distribution. The 'map_single_fragments.py' script uses the bwa alignment program (9) in paired-end mode and allowing for 2 mismatches and a maximum insert size of 1500 bp. Fragments were classified as "single" and "chimeric"; chimeric reads were defined as having the individual reads mapping on different strands or mapping at a distance greater than 1000 bp apart if the reads were on the same strand. Following this classification, chimeras were assessed for significance by dividing the genome into non-overlapping windows (100 nt in length) and counting the number of mapped chimeras in each possible window-pair. The three replicates were assessed for and found to be reproducible (6, 10), and were merged into a single, unified dataset for exponential phase and a single, unified dataset for the stationary phase samples (Figure S9). Fisher's exact test was used to identify chimeric fragments that were significantly overrepresented than expected at random based on the number of single and chimeric fragments mapping to each region ($p \leq 0.05$ following

Bonferroni correction). The default output from the RIL-seq pipeline accepts any S-chimera that is sequenced ≥5 times. To apply a more stringent cut-off value, we only accepted those chimeras that were sequenced more frequently than 90% of the chimeras in the control experiment (i.e., wild-type PAO1 lacking the Hfq-V allele) for each growth phase. We thus retained only those S-chimeras with greater than 31 sequenced fragments for the exponential phase sample and more than 27 sequenced fragments for the stationary phase samples (Dataset S1). For each RNA of the resulting S-chimeras, we assigned the read to the corresponding gene in the PAO1 genome. S-chimeras that appear to arise from a single transcript but map at positions greater than 1000 bp apart were removed from the final S-chimera table; these potentially self-transcript derived S-chimeras are listed in Dataset S1.

Generation of Circos Plots.
The Circos plots depicted in Fig. 1D and SI Appendix, Fig. S3 were generated with the Circos software package version 0.69 (11). Briefly, all chimeric interactions containing the indicated RNAs were plotted for each experimental dataset (Exp. Phase and Stat. Phase) and colored as indicated in the legend for Fig. 1D. Figure S3 depicts the full set of S-chimeras for exponential phase (Fig. S3A) and stationary phase (Fig. S3B). S-chimeras comprised of two distinct sRNAs were plotted on top and are blue in color. The weight of the links connecting sRNA:sRNA S-chimeras is scaled based on the number of interactions observed for that particular S-chimera.

Determining relative abundance of sRNAs on Hfq & in total RNA.
For Fig. 1F, the relative abundance of each sRNA identified in all chimeras was calculated for each RIL-seq dataset (Exp. Phase and Stat. Phase) by dividing the number of chimeric fragments containing a particular sRNA by the total number of chimeric fragments containing sRNAs as described previously (12). In the instance where chimeric fragments involved sRNA-sRNA interactions, the chimera was counted twice and the total number of interactions was updated accordingly. To assess the relative abundance of sRNAs co-purifying with Hfq in our RIL-seq experiment, we analyzed the initial alignment files from the RIL-seq pipeline (i.e., those generated by the 'map_single_fragments.py' script in the RIL-seq distribution) by using htseq-count (13) to assign the mapped reads to genes in the PAO1 genome. The counts were then normalized by the total number of fragments mapped for each dataset (exponential phase and stationary phase, respectively). sRNA annotations were ranked by relative abundance in each replicate, and the average abundance across the three replicate datasets was used to generate the pie charts depicted in Figure S4 panels A and B. For determining the relative abundance of sRNAs in the Total RNA-seq samples, sequencing reads from the Total RNA libraries generated from the RIL-seq samples were mapped to the PAO1 genome using bowtie2, counted with htseq-count and analyzed with DESeq2 in R (14). Relative sRNA abundance in each growth phase (i.e., Hfq-V and PAO1 in exponential phase and Hfq-V and PAO1 in stationary phase) was determined using the 'baseMean' value (the mean of normalized counts for all samples in the dataset) and are plotted in Figure S4 panels C and D.

MEME analysis of RIL-seq RNAs.
Binding motifs for the Hfq-interacting RNAs were searched using MEME software (15). The chimeric fragment pairs were separated into RNA1 and RNA2 fragments and any overlapping fragments were merged into a single genomic region. A 50-bp window was added to each side of the fragment, except for fragments classified as sRNAs, for which the full sRNA sequence was used. The nucleotide sequence for each unique RNA identified was extracted from the PAO1 genome and used as input for the MEME algorithm. Output was restricted to search only the given strand with a maximum length of 15 nucleotides, and zero or one occurrences were allowed for a maximum of 10 sequence logos.

Extraction of chimeras with PhrS as RNA2.
Chimeras containing PhrS (for panels in Fig. 2 and Fig. 4) were created by first extracting all chimeric fragments containing reads mapping to PhrS from the full Stationary Phase RIL-seq dataset based on genomic coordinates. We then used the 'generate_BED_file_of_endpoint.py' script included with the RIL-seq distribution to create a BED file of the PhrS-containing chimeras. The BED files were subsequently converted to the bam format using bedtools (16) to facilitate visualization in IGV (17).

RNA Isolation. RNA was extracted with TriReagent LS (Sigma-Aldrich) according to the manufacturer's recommendations. Briefly, cell pellets (collected as described in sections below) were homogenized in 1 mL of room temperature TriReagent, incubated at room temperature for 5 minutes, mixed vigorously with 100 µL 1-bromo-2-chloropropane (Sigma-Aldrich) and incubated at room temperature for 10 minutes. Samples were then centrifuged at full speed in a tabletop centrifuge for 15 minutes at 4˚C and the aqueous layer (≈ 0.6 mL) was transferred to a fresh tube. Nucleic acids were precipitated via the addition of 0.5 mL isopropanol, mixed by

inversion, and incubated at room temperature for 10 minutes prior to centrifugation for 10 min at 4˚C at full speed. The resulting RNA pellets were washed with 1 mL freshly prepared 75% ethanol, air-dried for ≈15 min at room temperature and hydrated in 20-50 µL nuclease free water. RNA was routinely quantified via NanoDrop (ThermoFisher Scientific).

RNA-sequencing. Sequencing for the PhrS pulse-expression experiment was performed by SeqCenter (Pittsburg, PA). Quality control and adapter trimming was performed with bcl2fastq. Read mapping was performed with bowtie2 version 2.4.5 using the very-sensitive setting along with the following options: no-mixed, no-unaligned, no-discordant, dove-tailing allowed (18). Read quantification was performed with htseq-count version 2.0.2. (13). Differential gene expression analysis was conducted with DESeq2 (14). The volcano plot depicted in Figure 3A was generated using the R package EnhancedVolcano (19).

Northern Blot Analysis. For the growth-curve Northern blot experiment depicted in SI Appendix, Fig. S2, PAO1 and PAO1 Δ*hfq* cells were grown overnight in NCE-succinate medium (3) and back-diluted to a starting density of 0.05 OD_{600} in 220 mL LB. At the indicated times, RNA was extracted from the equivalent of 10 OD units. For the northern blots depicted in Figures 2 and 4, overnight cultures of the indicated strains were back-diluted 1:300 into fresh LB medium containing gentamicin (30 µg/mL) and arabinose (0.2% w/v) and grown for 6 hours, at which time RNA was extracted from 2 mL of the culture. For the northern blot experiment depicted in SI Appendix, Fig. S7, overnight cultures of the indicated strains were back-diluted into LB containing gentamicin (30 µg/mL) to a starting density of 0.01 OD_{600} and grown at 37˚C for 6 hours at which point arabinose was added to a final concentration of 0.2% (w/v) and grown for an additional 20 minutes. RNA was extracted from 2 mL of the resulting culture.

Following RNA extraction, 5 µg of RNA were fractionated on 8% polyacrylamide urea gels containing 6 M urea (1:4 mix of Ureagel Complete to UreaGel-8 (National Diagnostics) with 0.08% Ammonium Persulfate) in 1X TBE buffer at 300 V for 75 minutes. RNA was subsequently transferred to a Zeta-Probe GT membrane (Bio-Rad) at 20V for 16-20 hr in 0.5X TBE. Following transfer, RNA was crosslinked to the membrane via UV irradiation. Size standards (RNA low-range ladder; NEB cat. no. N0364S) were marked using UV-shadowing. Membranes were blocked in ULTRAhyb-Oligo Hybridization Buffer (Ambion cat. no. AM8663) for 2 hr at 45˚C. Oligonucleotide probes (see Supplementary Table S4) were 5' ^{32}P-end labeled with 0.3 mCi of γ-^{32}P ATP (Perkin Elmer cat. no. NEG035C010MC) using 10 U of T4 polynucleotide kinase (NEB, cat. no. M0201) at 37˚C for 1 hr. Labeled probes were purified using Cytiva MicroSpin G-50 columns (Cytiva cat. No. 27-5330-01). 40 pmol of the radiolabeled probes were added to the blocked membranes and incubated overnight at 45˚C. The membranes were then washed twice with 2X SSC buffer/0.1% SDS at room temperature and thrice with 0.2X SSC buffer/0.1% SDS at room temperature, with the exception of the second wash, which was for 25 minutes at 45˚C. Northern blots were imaged using Carestream BioMax MR film (Sigma-Aldrich cat. no. Z350397) or captured on phospho-storage screens and imaged with an Azure Sapphire PhosphoImager. As needed, blots were stripped by three, 10 min incubations in boiling 0.2% SDS, and three, 10 min incubations in boiling water. Northern blots were repeated with two biological replicates and results from a single representative experiment are shown.

Beta-galactosidase Assays. Beta-galactosidase assays were conducted essentially as described previously (20). PAO1 and/or PAO1 Δ*phrS* cells were transformed with both the indicated *lacZ* reporter plasmid (derivatives of pME6014 (translational fusions) or pME6016 (transcriptional fusions) and the sRNA expression plasmid, pKH6, or derivatives thereof. Three individual colonies of the resulting transformants were grown overnight in LB containing tetracycline (35 µg/mL) and gentamicin (30 µg/mL) and subsequently back-diluted 1:300 in 3 mL of the same media containing arabinose (0.2% w/v) to induce expression from the arabinose-inducible promoter on pKH6. Cultures were grown with shaking at 37˚C for 6 hours (OD_{600} ≈ 1.5 – 2.0), after which time the cultures were incubated on ice for 20 minutes. 200 µL of culture were mixed with 800 µL of Z-buffer and permeabilized by the addition of 30 µL 0.1% SDS and 60 µL chloroform and assayed for β-galactosidase activity using 2-nitro-phenyl β-D-galactopyranoside (ONPG). Reactions were quenched with Na_2CO_3 and Miller units were calculated using OD_{420} and OD_{550} values (20). Values reported are the average of biological triplicate cultures with error bars representing one standard deviation. Statistical analyses were performed using one-way analysis of variance (ANOVA) followed by Bonferroni correction. All ß-gal experiments were repeated independently at least two times and results depict a single representative experiment.

Quantitate Reverse Transcriptase PCR (qRT-PCR). qRT-PCR was performed using cDNA derived from RNA collected from the indicated strains. Briefly, overnight cultures were back-diluted to a starting OD_{600} of 0.01 in fresh growth medium (LB + 30 µg/ml gentamicin and 0.02% w/v arabinose) and allowed to grow for 6 hours. Following the out-growth period, RNA from 2 mL of culture was collected as described above using TriReagent. The RNA was treated with RQ1 DNAse (Promega) and re-extracted. cDNA was synthesized using SuperScript IV (Thermo Fisher). 10 ng of the resulting cDNA were used as template for the qRT-PCR reactions using iTaq Universal SYBR Green SuperMix (Bio-Rad cat. no. 1725122) and an ABI QuantStudio 3 instrument (Applied Biosystems). Primer efficiencies were calculated for each target gene via serial dilutions and melting curve analyses. Data analysis was supported by the QuantStudio software. Transcript abundance was measured relative to the abundance of the *clpX* transcript. Relative transcript abundance values shown are the mean from all data points from two independent experiments and were calculated via the comparative threshold cycle (C_T) method ($2^{\wedge-\Delta\Delta CT}$) (21). qRT-PCR experiments were completed with biological triplicate cultures at least twice on independent samples; data from a single representative experiment are shown. Error bars represent one standard deviation of the mean. Results were analyzed for significance using ANOVA with Bonferroni correction.

Western Blotting. For the AntR-V western blot, overnight cultures of the indicated strains were back-diluted to an optical density (OD_{600}) of 0.01 in fresh LB and grown at 37˚C with shaking for 18 hours, at which time 100 µL of cells were pelleted and dissolved in 1X NuPAGE LDS Sample Buffer (Thermo Fisher cat. no. NP0007). Proteins were resolved by SDS-PAGE on 4-12% Bis-Tris NuPAGE gels (Thermo Fisher cat. no. NP0321) in MOPS running Buffer (Thermo Fisher cat. no. NP0001) and transferred to Immobilon-PSQ polyvinylidene fluoride (PVDF) membranes (EMD Millipore cat. no. ISEQ08100) using an XCell-II Blot Module (Thermo Fisher). Membranes were blocked in a 1:5 dilution of Blocking Buffer (LI-COR cat. no. 927-70001) for 1 hour prior to being probed with anti-VSV-G antibodies (Sigma Aldrich, cat. no. V4888) at a 1:3,333 dilution. Membranes were subsequently washed, blocked, and incubated with donkey anti-rabbit secondary antibodies conjugated with the near-infrared dye 800CW (LI-COR cat. no. 925-32213) at a dilution of 1:10,000. Imaging was performed on an Azure C600 imaging system (Azure Biosciences). Data from a single, representative replicate are shown and the experiment was performed independently at least two times with biological triplicates.

Measurement of Pyocyanin and *Pseudomonas* Quinolone Signal (PQS). Pyocyanin production was determined as previously described (22, 23). Triplicate overnight cultures of the indicated strains were refreshed into 200 mL LB at an optical density (OD_{600}) of 0.05. Samples (5 mL at each time point) for measuring pyocyanin production were collected at 6, 16, and 24 hours post refresh. The samples were centrifuged at 4,000 x g for 10 minutes and the resulting supernatants were mixed with 3 mL of chloroform, vortexed and the phases allowed to separate. The upper aqueous layer was removed and 1 mL of 0.2 N hydrochloric acid was added to the lower organic phase and vortexed. The organic/aqueous phases were allowed to separate again. Pyocyanin concentrations were determined based on the OD_{520} of the upper aqueous layer (Pyocyanin in µg/mL = OD_{520} x 17.072). Extraction and measurement of PQS was performed essentially as described previously (24). Briefly, overnight cultures of the indicated strains were back diluted into 200 mL of LB to an initial optical density (OD_{600}) of 0.05. The refreshed cultures were grown for 24 hours, at which point 2 mL of the culture was removed, centrifuged at full speed (~ 21,000 x g) for 1 min. The resulting supernatant was subsequently filtered through a 0.2 µm syringe filter. 500 µL of the filtered supernatant was transferred to a fresh Eppendorf tube and mixed with 500 µL of acidified ethyl acetate (10 mL ethyl acetate with 1.5 µL glacial acetic acid) by vortexing for 30 seconds. After phase separation, the top layer was collected and the ethyl acetate extraction was repeated again on the remaining bottom layer. Following the second extraction, the two upper layers were combined, dried by speed vac at 45˚ C for approximately 25 minutes. The resulting pellets were solubilized in in 20 µL methanol, 2 µL of each sample was spotted on TLC plates (20 cm x 20 cm Silica 60 F254 TLC plates; Merck product number 1055700001; TLC plates were pre-treated by soaking in 5% K_2HPO_4 for 30 min and activated at 100°C for 1 hour) and resolved in a TLC chamber in 95:5 dichloromethane: methanol solvent until the solvent front reached the top of the chamber. As a control, 1 µL of 10 mM synthetic PQS (Sigma-Aldrich product number 74398-10mg) was also spotted on the TLC plate. The TLC plates were visualized under UV light and the relative amounts of PQS was quantified using ImageJ. Pyocyanin and PQS experiments were repeated at least twice with independent biological triplicate cultures. Data presented in Supplemental Figure S8 are from a single, representative experiment.

Supplemental Figures

Figure S1

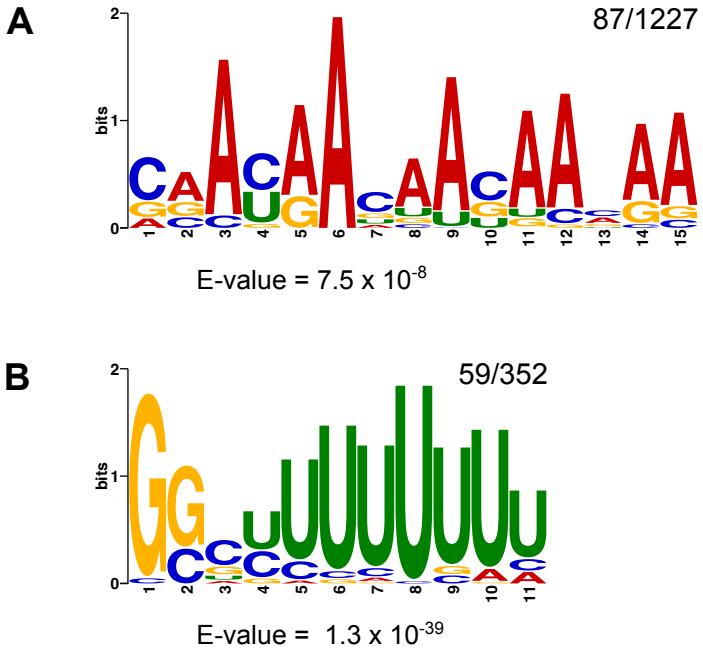

Figure S1. Motif analysis of RNAs identified in the RIL-seq experiment. Common motifs identified in each read position of the RIL-seq chimeras for all unique RNA1 RNAs (A) and all unique RNA2 RNAs (B). Motifs and E-values were determined by MEME (25). Fractions indicate the number of sequences containing the motif over the total number of unique RNAs identified in each position.

Figure S2

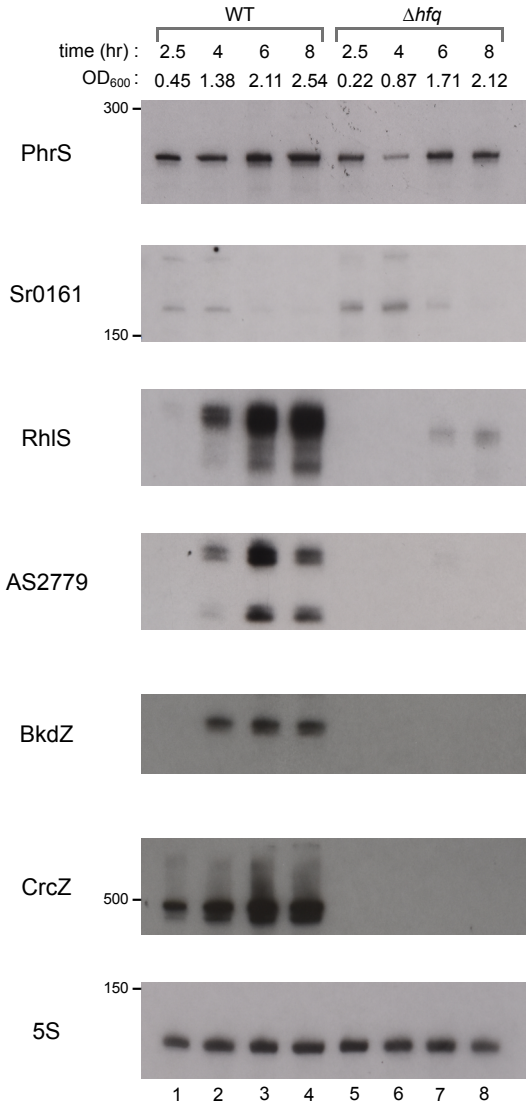

Fig. S2. Abundance of select sRNAs as a function of growth in wild-type PAO1 (WT) and PAO1 Δ*hfq* mutant (Δ*hfq*) cells. The strains were grown in LB medium and RNAs collected at 2.5 hours (lanes 1, 5), 4 hours (lanes 2, 6), 6 hours (lanes 3, 7), and 8 hours (lanes 4, 8) of growth were separated on polyacrylamide gels and subjected to northern blot analysis using radiolabeled oligonucleotides specific to the indicated RNA species on the same membrane. Size markers are in nt. Lanes 1-4, RNA collected from WT cells. Lanes 5-8, RNA collected from Δ*hfq* cells. OD_{600} values indicate the culture density at the time of collection. We note that the stability of PhrS is known to be unaffected by inactivation of Hfq and the effect of Hfq on the abundance of Phrs is evidently due to reduced levels of the transcription regulator Anr (26).

Figure S3

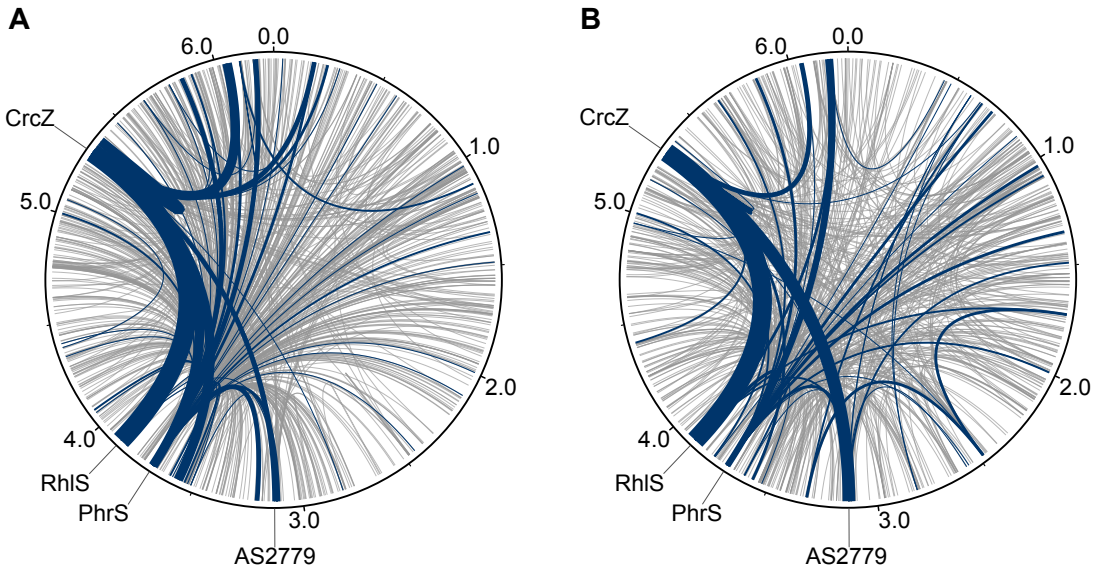

Fig. S3. Rewiring of the sRNA-sRNA interaction network occurring on Hfq in *P. aeruginosa* upon growth phase transition. Circos plots (11) depict S-chimeras detected in exponential phase (A) and stationary phase (B). S-chimeras comprised of sRNA-sRNA interactions are plotted in blue, with the thickness of the lines connecting two sRNAs scaled according to the total number of interactions detected for that particular S-chimera. S-chimeras comprised of other types (i.e., non-sRNA-sRNA interactions) are colored in grey.

Figure S4

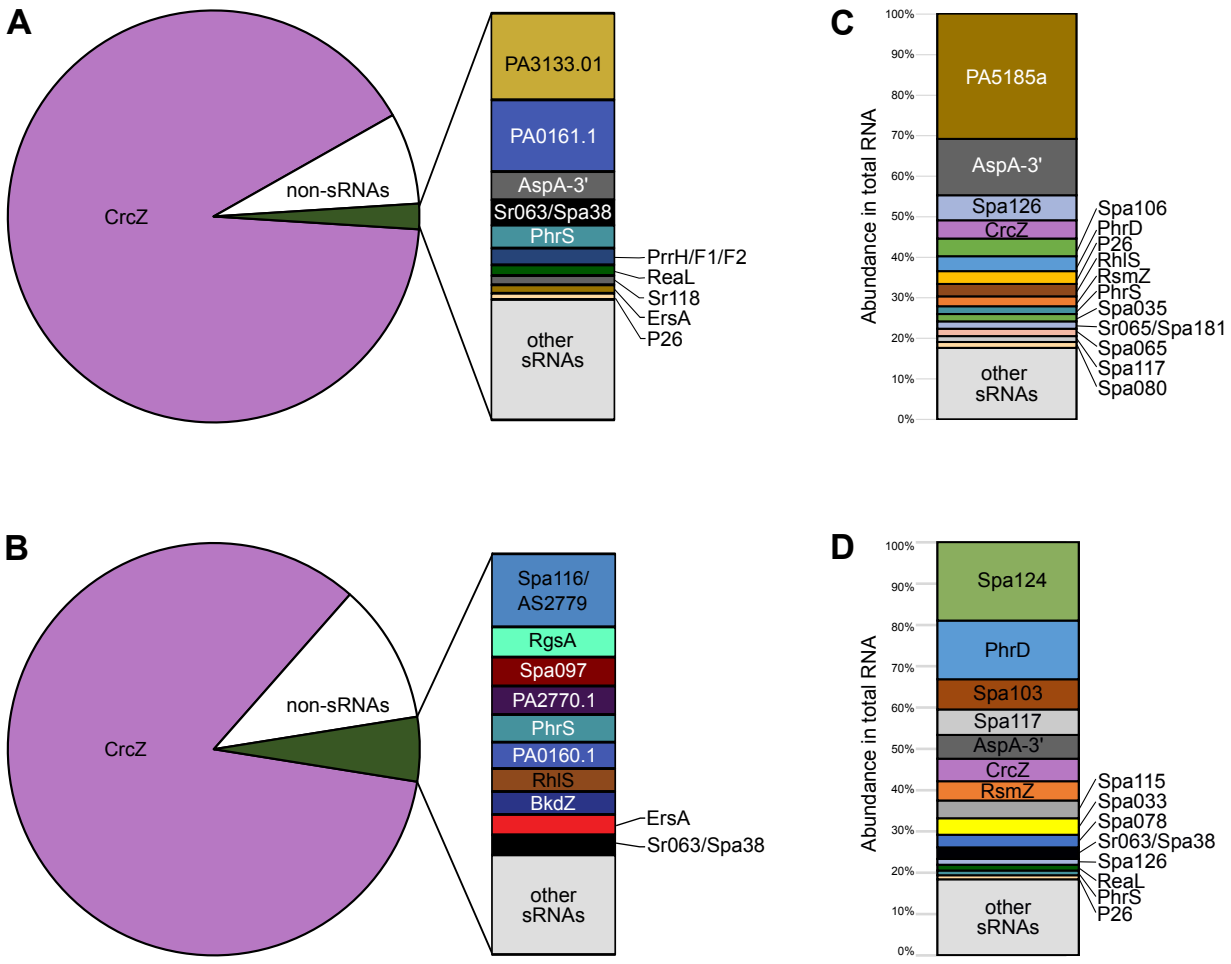

Fig. S4. Relative abundance of RNA species on Hfq (panels A, B) and in total RNA (panels C, D) in *P. aeruginosa*. (A, B) RNAs interacting with Hfq as single fragments (i.e., non-chimeric RNAs) were mapped to their corresponding genomic location. Plots in A and B depict the 11-most prevalent sRNA species identified in exponential phase (A) and stationary phase (B), as well as the fraction of single fragments corresponding to the remaining sRNA (other sRNAs) and non-sRNA species (non-RNAs). (C, D) The relative abundance amongst all detected sRNAs are plotted as a stacked bar chart for the total RNA-seq transcriptomes for exponential phase (C) and stationary phase (D). Data in C and were generated by DESeq2 analysis of the total RNA-seq transcriptomes collected from the pre-IP RNA samples used in the RIL-seq experiment.

Figure S5

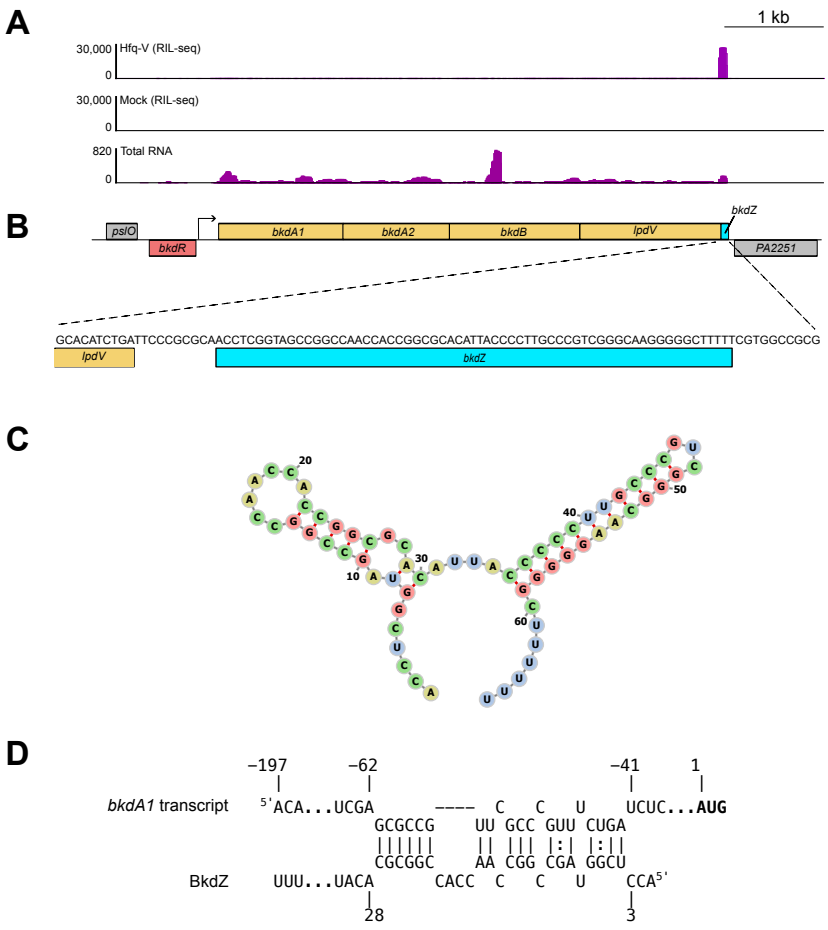

Fig. S5. BkdZ is an sRNA derived from the 3′-UTR of *lpdV*. (A) RIL-seq panels: Reads from RIL-seq with PAO1 Hfq-V cells (Hfq-V) grown to stationary phase compared to RIL-seq with wild-type cells (Mock) that do not synthesize any epitope-tagged Hfq. Total RNA panel: Total RNA-seq reads from PAO1 Hfq-V cells grown to stationary phase. Only reads corresponding to the plus strand are shown. (B) Genomic context of BkdZ. The arrow indicates the presumptive transcription start site as determined by (27). (C) Structure prediction of BkdZ using RNAfold version 2.4.18 (28). (D) IntaRNA (29) prediction of base-pairing between between BkdZ and the 5' untranslated region of the *bkdA1* mRNA. Upper numbers indicate the position relative to the *bkdA1* start codon (indicated by bold text); lower numbers indicate nt position in BkdZ.

Figure S6

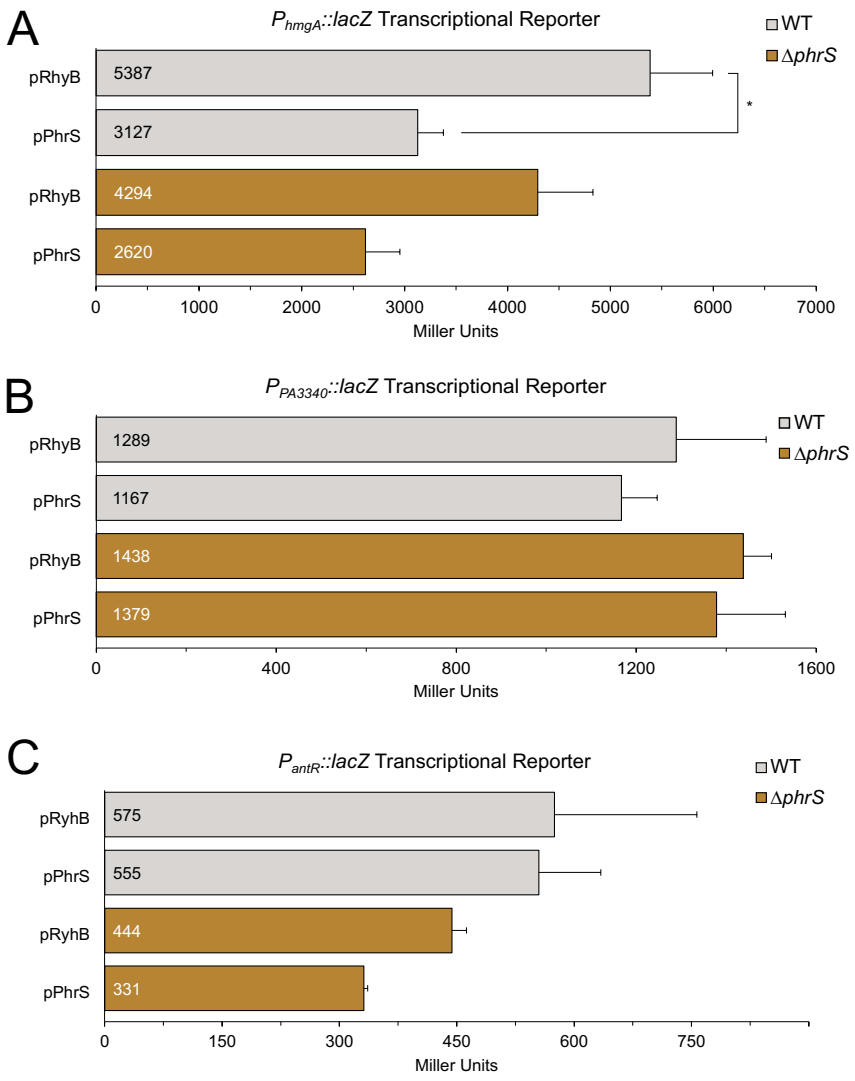

Fig. S6. PhrS does not appreciably alter the activity of *hmgA*-, *PA3340*-, or *antR-lacZ* transcriptional fusions. β-Galactosidase activity (in Miller Units) of PAO1 WT cells (in gray) or PAO1 Δ*phrS* mutant cells (in brown) containing *hmgA-lacZ* (A), *PA3340-lacZ* (B), or *antR-lacZ* (C) transcriptional fusions and the indicated plasmids. Plasmid pPhrS encodes PhrS, pRyhB encodes the *E. coli* sRNA RyhB. Assays were conducted with biological triplicate cultures and repeated independently at least twice. Data shown from a single representative experiment with error bars representing one standard deviation of the mean. Significance was assessed by one-way ANOVA with Bonferroni post-test correction. Asterisks indicate significant differences with p-value ≤ 0.05 (*).

Figure S7

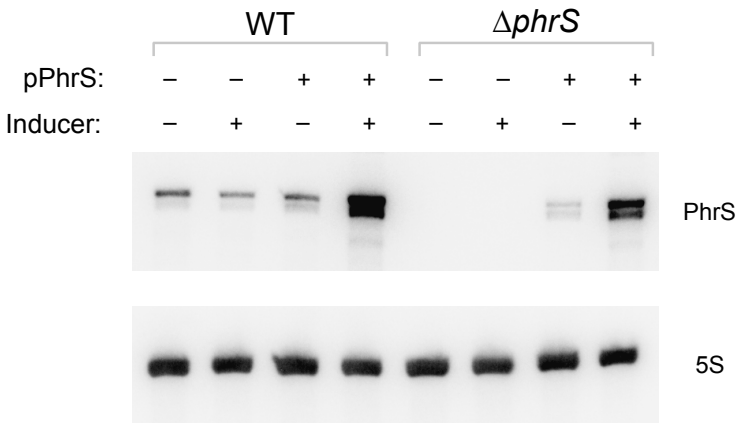

Fig. S7. Northern blotting for pulse-expression of PhrS from plasmid pPhrS. PAO1 wild-type cells (WT) or PAO1 Δ*phrS* mutant cells (Δ*phrS*) harboring the indicated plasmids were grown to stationary phase (OD_{600} ≈ 2.0) and were either treated or not treated to arabinose at a final concentration of 0.2% (w/v) for 20 minutes, as indicated. Following the 20-minute treatment period, RNAs were extracted from 2 mL of each culture, separated on polyacrylamide gels, and subjected to northern blot analysis using radiolabeled oligonucleotides specific to the indicated RNA species on the same membrane.

Figure S8.

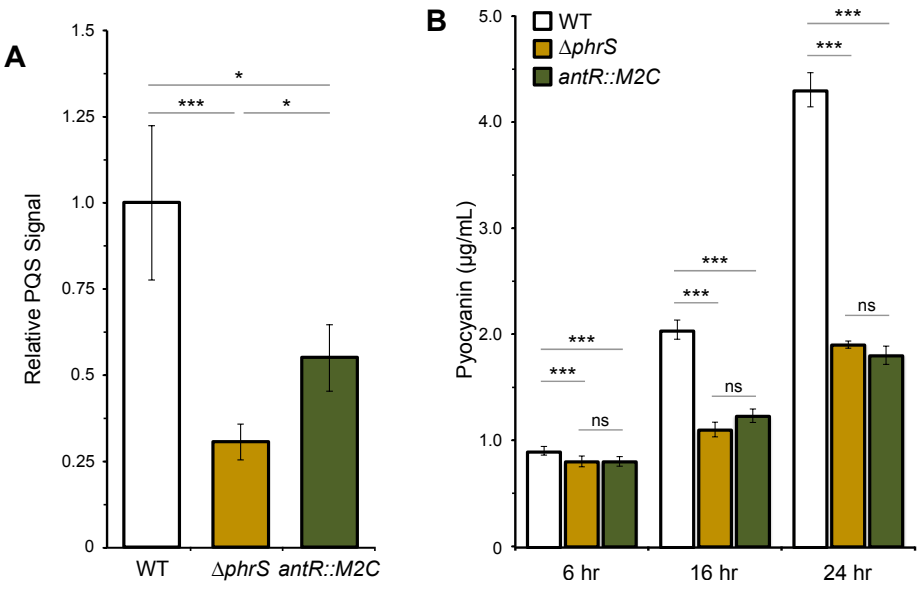

Fig S8. PhrS regulates PQS and Pyocyanin through AntR. Overnight cultures of wild-type PAO1 (WT), PAO1 Δ*phrS* (Δ*phrS*), and PAO1 *antR::M2C* (*antR::M2C*), which harbors the M2C mutation that is predicted to disrupt the interaction between PhrS and the *antR* mRNA, were refreshed into LB medium to an OD_{600} of 0.05 and grown for 24 hour for PQS production (A) or for the indicated times for pyocyanin measurements (B). PQS and Pyocyanin experiments were repeated at least twice with independent cultures. Data presented are from a single experiment and displayed are the mean values from biological triplicates. Error bars represent one standard deviation. Significance was assessed by ANOVA with Bonferroni correction; ns, not significant; *, $p \leq 0.05$; *** $p \leq 0.001$.

Figure S9

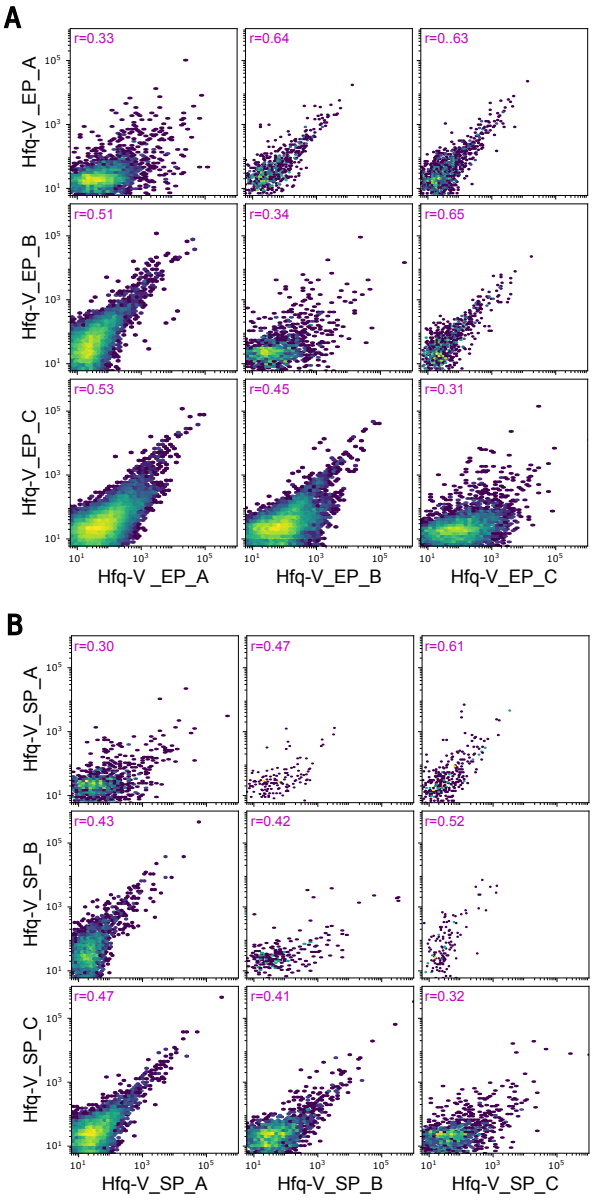

Fig. S9. Assessment of RIL-seq dataset reproducibility. The reproducibility of results amongst the replicate datasets for exponential phase (A) and stationary phase (B) was evaluated as described previously (10). Sequenced fragments were binned into 100 nt windows across the genome with each point in the plot represening the number of fragments mapped to a given region. The color is scaled from blue (small number of fragments) to yellow (high number of fragments). The plots positioned above the diagonal (i.e., the three plots on the upper right) represent reproducibility amongst the S-chimeras (i.e., significant chimeric fragments) in each dataset; plots positioned along the diagonal represent intra-library comparisons between single and chimeric fragments; plots positioned below the diagonal (i.e., the three plots on the lower left) represent single fragments. The Spearman correlation coefficients (r) are reported for each scatter plot.

Supplemental Figures

Table S1. Candidate sRNAs identified by RIL-seq.

sRNA name	Locus tag	Strand	Start	Stop
PA0160.1	PA0160.1	+	184011	184112
PA0217-5'	PA0217.1	-	245678	245752
GabT-3'	PA0266.1	+	302517	302588
SahHas[a]	PA0432.1	+	483071	483179
PA0806.1	PA0806.1	-	884182	884254
QuiP-3'	PA1031.1	-	1119579	1119644
FlgDas[a]	PA1079.1	-	1165473	1165555
PA1507-3'	PA1506.1	-	1636260	1636329
BkdZ	PA2250.1	+	2478180	2478255
OprN-3'	PA2495.1	+	2814616	2814687
PA3133.01	PA3133.01	-	3514661	3514722
PA3181-3'	PA3180.1	-	3570899	3570964
OprB-3'	PA3185.1	-	3575845	3575911
AzoR3-3'	PA3222.1	-	3611198	3611291
PA3449.1	PA3449.1	-	3855364	3855443
AceF-3'	PA5016.1	+	5640609	5640682
NtrC-3'	PA5125.01	+	5774772	5774859
PA5185as[a]	PA5185.1	+	5837811	5837971
BetT1-5'	PA5374.1	+	6051423	6051570
BetZ	PA5375.1	+	6053199	6053266
AspA-3'	PA5429.1	+	6110758	6110937

[a] as, anti-sense sRNAs transcribed on the opposite strand of another gene

Table S2. Bacterial strains used in this study.

Bacterial Strains	Source
Escherichia coli DH5α F′IQ	ThermoFisher
Escherichia coli SM10 (λpir)	Arne Rietsch (Case Western University)
Pseudomonas aeruginosa PAO1	Arne Rietsch (Case Western University)
PAO1 Hfq-V	(3)
PAO1 Δ*phrS*	(3)
PAO1 Δ*hfq*	(3)
PAO1 *antR-V*	This study
PAO1 *M2C antR-V*	This study
PAO1 *phrS-SM179 M2C antR-V*	This study

Table S3. Plasmids used in this study.

Plasmid	Description	Source
pKH6	Empty vector for sRNA expression	(2)
pRyhB	pKH6 with RyhB sRNA from *E. coli*	This study
pPhrS	pKH6-PhrS	(3)
pPhrSΔseed	pKH6-PhrS lacking nucleotides 170-181	This study
pPhrSΔ1/2seed	pKH6-PhrS lacking nucleotides 175-181	This study
pPhrS-mini	pKH6-PhrS nucleotides 161-213	This study
pPhrS-SM171	pKH6-PhrS allele with CG at position 171-172	This study
pPhrS-SM172	pKH6-PhrS allele with GT at position 172-173	This study
pPhrS-SM173	pKH6-PhrS allele with TG at position 173-174	This study
pPhrS-SM174	pKH6-PhrS allele with GC at position 174-175	This study
pPhrS-SM175	pKH6-PhrS allele with CG at position 175-176	This study
pPhrS-SM176	pKH6-PhrS allele with GT at position 176-177	This study
pPhrS-SM177	pKH6-PhrS allele with TT at position 177-178	This study
pPhrS-SM178	pKH6-PhrS allele with TC at position 178-179	This study
pPhrS-SM179	pKH6-PhrS allele with CC at position 179-180	This study
pPhrS-SM180	pKH6-PhrS allele with CG at position 180-181	This study
pPhrS-SM181	pKH6-PhrS allele with GT at position 181-182	This study
pPhrS-SM182	pKH6-PhrS allele with TG at position 182-183	This study
pME6014	Empty vector for translational *lacZ* fusions	(4)
pME6016	Empty vector for transcriptional *lacZ* fusions	(4)
pME6014-*hmgA*	Translational *lacZ* fusion for *hmgA*	This study
pME6014-*hmgA-SMC175*	Translational *lacZ* fusion for *hmgA* with compensatory mutations to restore interaction with *phrS-SM175* allele	This study
pME6016-*hmgA*	Transcriptional *lacZ* fusion for *hmgA*	This study
pME6014-*PA3340*	Translational *lacZ* fusion for *PA3340*	This study
pME6016-*PA3340*	Transcriptional *lacZ* fusion for *PA3440*	This study
pME6014-*antR*	Translational *lacZ* fusion for *antR*	This study
pME6014-*antR-M2C*	Translational *lacZ* fusion for *antR* with compensatory mutations to restore interaction *phrS-SM179* allele	This study
pME6016-*antR*	Transcriptional *lacZ* fusion for *antR*	This study
pEXG2	Allele exchange vector	(4)
pEXG2.Δ*phrs*	Deletion of *phrS* from chromosome	(3)
pEXG2.*antR-V*	Introduction of *antR::VSVG* into chromosome	This study
pEXG2.*phrS-SM179*	Introduction of *phrS-SM179* into chromosome	This study
pEXG.*antR-M2C*	Introduction of *antR-M2C* mutation into chromosome	This study

Table S4. Oligonucleotide primers used in this study.

Primer Name/Function	Sequence (5' -> 3')[a]	Source
lacZ reporter constructs		
*hmgA*_reporters_fwd	agaatggcaaaagcttcgaattcGCAGGAACGCGGCGAACA	This study
*hmgA*_translational_rev	acgacgggagcaagcttggctgcagCGCTGCTGAATTCGTTGCCG	This study
*hmgA*_transcriptional_rev	gttatccgctcacaattctgcagCGCATAACGTAATTTGAGTGGAAGGCAG	This study
*hmgA-SM175C*_rev	GGACCTGGCAC***CG***TGGCTGCGTTAT	This study
*hmgA-SM175C*_fwd	ATAACGCAGCCA***CG***GTGCCAGGTCC	This study
*PA3340*_reporters_fwd	tgagaatggcaaaagcttcgaattcCCCAAGGCCGATGTGCTGAT	This study
*PA3340*_translational_fwd	ttgttatccgctcacaattctgcagGCCCGAATTTCGCCCCGTA	This study
*PA3340*_transcriptional_rev	acgacgggagcaagcttggctgcagGGCACGACCAGGCACACAA	This study
*antR*_reporters_fwd	tgagaatggcaaaagcttcgaattcTGCCTTCCTCGGGACGGA	This study
*antR*_translational_rev	ttgttatccgctcacaattctgcagCTCCCCGCATCCTCCACTATC	This study
*antR*_transcriptional_fwd	acgacgggagcaagcttggctgcagCGGCATGGAGATCGCCAC	This study
qRT-PCR Primers		
*clpX*_fwd	TGCGATTACGATGTGGAGA	(30)
*clpX*_rev	CCCTCGATGAGCTTCAGCA	(30)
*antR*_fwd	CGTGCTGAAGTCGATGTG	This study
*antR*_rev	CAGGCTGTAGGCGTTGA	This study
*antA*_fwd	GAAGGCATCTTCCGCATC	This study
*antA*_rev	CTGGCCAGTTCGCTTTC	This study
*antB*_fwd	GATCCGAAGCGCGAGAC	This study
*antB*_rev	TGCGGATACGGAACACC	This study
RyhB expression plasmid		
RyhB_fwd	tcgcaactctctactgtttctagatGCGATCAGGAAGACCCTCGCGGAGAAC CTGAAAGCACGACATTGCTCACATTGCTTCCAG	This study
RyhB_rev	ccgccaaaacagccacagtaagcttAAAAAAAAAGCCAGCACCCGGCTGG CTAAGTAATACTGGAAGCAATGTGAGCAATGTCGTGC	This study
pKH6-PhrS mutant alleles		
P1_PhrS_alleles	atcgcaactctctactgtttctagatATCGAGCAACACCCAACCGGC	This study
P2_PhrSΔseed	cgccctaagtgCTGTGTATCCGGGAGGATCAGCC	This study
P3_PhrSΔseed	tcccggatacacagCACTTAGGGCGACTTCGGTC	This study
PhrS-mini_fwd	atcgcaactctctactgtttctagatGATACACAGAGCACGCAAGGCA	This study
P2_PhrS_SM171-172	TCTGTGTATCCGGGAGGATCAGC	This study
P2_PhrS_SM173-182	GCTCTGTGTATCCGGGAGGATCA	This study
P3_PhrS-SM171	TGATCCTCCCGGATACACAGA***CG***ACGCAAGGCACTTAGGG	This study
P3_PhrS-SM172	TGATCCTCCCGGATACACAGAG***GT***CGCAAGGCACTTAGGG	This study
P3_PhrS-SM173	TCCTCCCGGATACACAGAGC***TG***GCAAGGCACT	This study
P3_PhrS-SM174	TCCTCCCGGATACACAGAGCA***GC***CAAGGCACTT	This study
P3_PhrS-SM175	TCCTCCCGGATACACAGAGCAC***CG***AAGGCACTTA	This study
P3_PhrS-SM176	TCCTCCCGGATACACAGAGCACG***GT***AGGCACTTAG	This study
P3_PhrS-SM177	TCCTCCCGGATACACAGAGCACGC***TT***GGCACTTAGG	This study
P3_PhrS-SM178	TCCTCCCGGATACACAGAGCACGCA***TC***GCACTTAGGG	This study
P3_PhrS-SM179	TCCTCCCGGATACACAGAGCACGCAA***CC***CACTTAGGGC	This study
P3_PhrS-SM180	TCCTCCCGGATACACAGAGCACGCAAG***CG***ACTTAGGGCGA	This study
P3_PhrS-SM181	TCCTCCCGGATACACAGAGCACGCAAGG***GT***CTTAGGGCGA	This study
P3_PhrS-SM182	TCCTCCCGGATACACAGAGCACGCAAGGC***TG***TTAGGGCGAC	This study
P4_PhrS_alleles	cgccaaaacagccactagtaagcttGCCGGTGTTTTTCCAGGCGC	This study
AntR-VSVG allele in chromosome		
P1_*antR-VSVG*	ggaagcataaatgtaaagcaagcttGCGCTGATCAAGGGACTGATCC	This study
P2_*antR-VSVG*	aggcggttcatttcgatgtcggtgtatgcggccgcGGAGCGCCGCGCAGCG	This study
P3_*antR-VSVG*	caccgacatcgaaatgaaccgcctgggcaagTGAGAGGGCGTTCAGGCGT	This study

P4_*antR-VSVG*	gtggaaattaattaaggtaccAGAGCGTGCTCAGCGAAGAG	This study
PhrS SM179 allele in chromosome		
P1_*phrS*-SM179_chrom	ggaagcataaatgtaaagcaagcttCCCAGCATCATTGGCAACATCAGG	This study
P2_*phrS*-SM179_chrom	GTCGCCCTAAGTG***GG***TTGCGTGCTCTGTGT	This study
P3_*phrS*-SM179_chrom	ACACAGAGCACGCAA***CC***CACTTAGGGCGAC	This study
P4_*phrS*-SM179_chrom	gtggaaattaattaaggtaccGAACAGCGCGATCATCAACACCG	This study
AntR-M2C allele in chromosome		
P1_*antR*_M2C	ggaagcataaatgtaaagcaagcttTGCCTTCCTCGGGACGGA	This study
P2_*antR*_M2C	TCGACACGGCAA***CC***CTGGGGGTGCG	This study
P3_*antR*_M2C	CGCACCCCCAG***GG***TTGCCGTGTCGA	This study
P4_*antR*_M2C	gtggaaattaattaaggtaccTCAGCTCCTGGCGCTCG	This study
Probes for Northern Blotting		
5S rRNA	CGTTTCACTTCTGAGTTCGGGAAGG	(31)
crcZ	GCTGGAGTCGTTACGTGTTG	(32)
rhlS	TGCGTGCTCTGTGTATCCGGGAGGATCAGC	(31)
phrS	CGATGAACATGTTGATGGCCTCCAGTTGCCGG	This study
sr0161	CACGTCCCGCTCTTGCATGGCGAGATCGAT	This study
AS2779	GCTGGTCGGGAAATACCCTTGGG	This study
bkdZ	CCCGACGGGCAAGGGGGTAATGTGCGC	This study

Notes

a: Nucleotides in lower-case indicate regions of homology added to facilitate cloning via isothermal assembly. Nucleotides in bold, italic, underlined font indicate the introduced mutations.

Table S5. gBlocks used in this study.

gBlocks	Sequence (5' -> 3')
pKH6.PhrS-Δ1/2seed	ATCGCAACTCTCTACTGTTTCTAGATATCGAGCAACACCCAACCGGCAACTGGAGGCCAT CAACATGTTCATCGACGAAGTGGTTCTCGCAGGGATTCTTACAGTAGGCCTCATGGTCG CTTTCTTCGGTGGGGTCGGTTACTTCATCTGGAAGGATTCCCATAGCCGCAAAGGCTGAT CCTCCCGGATACACAGAGCA***CA***CTTAGGGCGACTTCGGTCGCCCGTTTTTTTTGCGCCTG GAAAAACACCGGCAAGCTTACTAGTGGCTGTTTTGGCG

Dataset S1 (separate file). List of S-Chimeras from Exp. Phase and Stat. Phase RIL-seq libraries with greater than 32 (Exp. Phase) and 27 (Stat. Phase).

Dataset S2 (separate file). RNAseq data for PAO1 Δ*phrS* cells harboring plasmid pEV (empty vector pKH6) compared to PAO1 Δ*phrS* cells with plasmid pPhrS (pKH6.PhrS) or PAO1 Δ*phrS* cells with plasmid pPhrS-Δseed (pKH6.PhrS-Δseed) following a 20-minute pulse with 0.2% (w/v) final concentration of arabinose.

SI References

1. D. G. Gibson *et al.*, Enzymatic assembly of DNA molecules up to several hundred kilobases. *Nat. Methods.* **6**, 343-345 (2009).
2. K. Han, B. Tjaden, S. Lory, GRIL-seq provides a method for identifying direct targets of bacterial small regulatory RNA by in vivo proximity ligation. *Nat. Microbiol.* **2**, 16239 (2016).
3. T. K. Kambara, K. M. Ramsey, S. L. Dove, Pervasive Targeting of Nascent Transcripts by Hfq. *Cell Rep.* **23**, 1543-1552 (2018).
4. U. Schnider-Keel *et al.*, Autoinduction of 2,4-diacetylphloroglucinol biosynthesis in the biocontrol agent *Pseudomonas fluorescens* CHA0 and repression by the bacterial metabolites salicylate and pyoluteorin. *J. Bacteriol.* **182**, 1215-1225 (2000).
5. A. Rietsch, I. Vallet-Gely, S. L. Dove, J. J. Mekalanos, ExsE, a secreted regulator of type III secretion genes in *Pseudomonas aeruginosa*. *Proc. Natl. Acad. Sci. USA.* **102**, 8006-8011 (2005).
6. S. Melamed *et al.*, Mapping the small RNA interactome in bacteria using RIL-seq. *Nat. Protoc.* **13**, 1-33 (2018).
7. A. A. Shishkin *et al.*, Simultaneous generation of many RNA-seq libraries in a single reaction. *Nat. Methods.* **12**, 323-325 (2015).
8. M. Martin, Cutadapt removes adapter sequences from high-throughput sequencing reads. *EMBnet j.* **17**, 3 (2011).
9. H. Li, R. Durbin, Fast and accurate short read alignment with Burrows-Wheeler transform. *Bioinform.* **25**, 1754-1760 (2009).
10. S. Melamed *et al.*, Global Mapping of Small RNA-Target Interactions in Bacteria. *Mol. Cell.* **63**, 884-897 (2016).
11. M. I. Krzywinski *et al.*, Circos: An information aesthetic for comparative genomics. *Genome Res.* 10.1101/gr.092759.109 (2009).
12. S. Pearl Mizrahi *et al.*, The impact of Hfq-mediated sRNA-mRNA interactome on the virulence of enteropathogenic *Escherichia coli*. *Sci. Adv.* **7**, eabi8228 (2021).
13. S. Anders, P. T. Pyl, W. Huber, HTSeq--a Python framework to work with high-throughput sequencing data. *Bioinform.* **31**, 166-169 (2015).
14. M. I. Love, W. Huber, S. Anders, Moderated estimation of fold change and dispersion for RNA-seq data with DESeq2. *Genome Biol.* **15**, 550 (2014).
15. A. Valouev *et al.*, Genome-wide analysis of transcription factor binding sites based on ChIP-Seq data. *Nat. Methods.* **5**, 829-834 (2008).
16. A. R. Quinlan, I. M. Hall, BEDTools: a flexible suite of utilities for comparing genomic features. *Bioinform.* **26**, 841-842 (2010).
17. H. Thorvaldsdóttir, J. T. Robinson, J. P. Mesirov, Integrative Genomics Viewer (IGV): high-performance genomics data visualization and exploration. *Brief Bioinform.* **14**, 178-192 (2013).
18. B. Langmead, S. L. Salzberg, Fast gapped-read alignment with Bowtie 2. *Nat. Methods.* **9**, 357-359 (2012).

19. K. Blighe, S. Rana, M. Lewis (2022) EnhancedVolcano: Publication-ready volcano plots with enhanced couloruing and labeling. R package version 1.14.0, <https://github.com/kevinblighe/EnhhancedVolcano>. Access date: Nov 2, 2022.
20. M. J. Gebhardt, T. K. Kambara, K. M. Ramsey, S. L. Dove, Widespread targeting of nascent transcripts by RsmA in *Pseudomonas aeruginosa*. *Proc. Natl. Acad. Sci. USA.* **117**, 10520-10529 (2020).
21. K. J. Livak, T. D. Schmittgen, Analysis of relative gene expression data using real-time quantitative PCR and the 2(-ΔΔ C(T)) Method. *Methods.* **25**, 402-408 (2001).
22. D. W. Essar, L. Eberly, A. Hadero, I. P. Crawford, Identification and characterization of genes for a second anthranilate synthase in *Pseudomonas aeruginosa*: interchangeability of the two anthranilate synthases and evolutionary implications. *J. Bacteriol.* **172**, 884-900 (1990).
23. M. Malešević *et al.*, *Pseudomonas aeruginosa* quorum sensing inhibition by clinical isolate *Delftia tsuruhatensis* 11304: involvement of *N*-octadecanoylhomoserine lactones. *Sci. Rep.* **9**, 16465 (2019).
24. H. Hendrix *et al.*, Metabolic reprogramming of *Pseudomonas aeruginosa* by phage-based quorum sensing modulation. *Cell Rep.* **38**, 110372 (2022).
25. T. L. Bailey *et al.*, MEME SUITE: tools for motif discovery and searching. *Nucleic acids Res.* **37**, W202-W208 (2009).
26. E. Sonnleitner *et al.*, Detection of small RNAs in *Pseudomonas aeruginosa* by RNomics and structure-based bioinformatic tools. *Microbiol.* **154**, 3175-3187 (2008).
27. O. Wurtzel *et al.*, The single-nucleotide resolution transcriptome of *Pseudomonas aeruginosa* grown in body temperature. *PLoS Pathog.* **8**, e1002945 (2012).
28. A. R. Gruber, R. Lorenz, S. H. Bernhart, R. Neuböck, I. L. Hofacker, The Vienna RNA websuite. *Nucleic Acids Res.* **36**, W70-W74 (2008).
29. M. Mann, P. R. Wright, R. Backofen, IntaRNA 2.0: enhanced and customizable prediction of RNA-RNA interactions. *Nucleic Acids Res.* **45**, W435-W439 (2017).
30. S. Castang, H. R. McManus, K. H. Turner, S. L. Dove, H-NS family members function coordinately in an opportunistic pathogen. . *Proc. Natl. Acad. Sci. USA.* **105**, 18947-18952 (2008).
31. M. K. Thomason *et al.*, A *rhlI* 5' UTR-Derived sRNA Regulates RhlR-Dependent Quorum Sensing in *Pseudomonas aeruginosa*. *mBio* **10**, e02253-02219 (2019).
32. M. Gerovac *et al.*, A Grad-seq View of RNA and Protein Complexes in Pseudomonas *aeruginosa* under Standard and Bacteriophage Predation Conditions. *mBio* **12** (2021).